J. Biochem. **143,** 131–141 (2008)
doi:10.1093/jb/mvm201

Isolation, Characterization and Structure-Elicitor Activity Relationships of Hibernalin and its Two Oxidized Forms from *Phytophthora hibernalis* Carne 1925

Renato Capasso[1,*,†], Antimo Di Maro[2,†], Gennaro Cristinzio[3], Antonio De Martino[1], Angela Chambery[2], Addolorata Daniele[2], Filomena Sannino[4], Antonino Testa[3,5] and Augusto Parente[2]

[1]Dipartimento di Scienze del Suolo, della Pianta, dell' Ambiente e delle Produzioni Animali, Facoltà di Agraria, Università degli Studi di Napoli "Federico II", I-80055 Portici (NA); [2]Dipartimento di Scienze della Vita, Facoltà di Scienze Matematiche, Fisiche e Naturali, Seconda Università di Napoli, 81100 Caserta; [3]Dipartimento di Arboricoltura, Botanica e Patologia Vegetale, Facoltà di Agraria, Università degli Studi di Napoli "Federico II", 80055 Portici; [4]Dipartimento di Scienze del Suolo della Pianta dell' Ambiente e delle Produzioni Animali, Facoltà di Scienze Biotecnologiche, Università degli Studi di Napoli "Federico II" 80055 Portici; and [5]Istituto di Biotecnologie Biochimiche, Facoltà di Agraria, Università Politecnica delle Marche, Ancona, Italy

Received August 3, 2007; accepted October 14, 2007; published online October 30, 2007

Three α-elicitins, named hibernalin1, hibernalin2 and hibernalin3 (hib1, hib2 and hib3, respectively), were isolated by reverse phase-low-pressure liquid chromatography from culture filtrates of *Phytophthora hibernalis* Carne 1925, the causal agent of citrus lemon brown rot. Hib1 proved to be identical to syringicin previously isolated from culture filtrates of *Phytophthora syringae*. Hib2 and hib3 shared the same primary structure with hib1, but contained, at position 50, Met sulphoxide or sulphone, respectively. By SDS–PAGE, the three proteins showed the same electrophoretic mobility, corresponding to about 10 kDa. Exact M_r values were obtained by MALDI-TOF-MS (10,194.82 for hib1, 10,209.33 for hib2 and 10,223.80 for hib3), while by ESI-MS an M_r value of 10,194.90 was found for hib1 and no results for hib2 and hib3. The hibernalin forms showed a high propensity to self-association, after exposure to acetonitrile. Hib1 showed to be active in both the hypersensitivity response and electrolytes leakage assays; the sample containing hib1 and hib2 was only weakly active in the first assay and inactive in the second assay, while the sample containing all three hibernalin forms proved to be inactive in both tests. It is proposed that the different activities of the three hibernalin samples could be very likely attributed to both Met50 oxidation and aggregation.

Key words: amino acid sequence, biological activity, citrus lemon, hibernalins, Phytophthora hibernalis.

Abbreviations: hib1, hibernalin1; hib2, hibernalin2; hib3, hibernalin3; RP-LPLC, reverse phase-low-pressure liquid chromatography; HR, hypersensitivity response; Hse, homoserine; Hse, homoserine lactone; ELA, electrolytes leakage assay; PR, pathogenesis related; SAR, systemic acquired resistance; DFDNB, 1,5-difluoro-2,4-dinitrobenzene.

Phytophthora species are plant pathogens which attack numerous crops and woody plants. They produce protein elicitors generally named elicitins which are involved in the recognition of plant pathogens, inducing natural defense mechanisms of plants in non-host resistance (*1*). Elicitins are classified into α-class, acidic elicitins, with valine at position 13, and β-class, basic and more toxic elicitins, with hydrophilic residues at position 13 (*2*, *3*). They are small proteins of 98 amino acids, with M_r of about 10 kDa, isolated and purified from culture filtrates of several *Phytophthora* and *Pythium* species (oomycetes) (*4–14*). Elicitins induce hypersensitivity response (HR) (*15*) with the production of phytoalexins, ethylene (*16*) and pathogenesis related (PR) proteins, with consequent electrolyte leakage (*17*) and systemic acquired resistance (SAR) in tobacco and in some species of *Brassicaceae* (*18*).

Pythiaceae are not able to synthesize sterols (*19*), but their requirement for growth and both sexual and asexual reproductions is still subject to controversy (*20*)

It has been reported that elicitins are involved in sterol transport, as in the case of cryptogein, a α-elicitin produced by *Phytophthora cryptogea*, which binds to dehydroergosterol and catalyzes its transport between liposomes (*21*).

The elicitin-sterol complexes were proposed to be the active form able for the binding to elicitin receptors, located on plant plasma membrane (*22*), in an allosteric manner (*23*). The property of these proteins to load sterols has been exploited for the preparation of

*To whom correspondence should be addressed. Tel: +39 081 2539173, Fax: +39 081 2539186,
E-mail: renato.capasso@unina.it
†These authors contributed equally to this work.

anticholesteremic agents, and their medical use has been patented (*21*). Recent studies on plant defense relationships demonstrated that elicitins share some common structural and functional properties with lipid-transfer proteins, secreted by plant cells, being both able to load and transfer lipidic molecules. Furthermore, sharing also the same biological receptors, they likely play a key role in the lipid-mediated dialogue between the pathogen and the plant (*24*, *25*).

Phytophthora hibernalis Carne 1925 is the causal agent of citrus lemon brown rot disease, also known with the term of foot rot and collar rot. Foot rots caused by *Phytophthora* spp. continue to be primary factors in poor growth and death of citrus trees of all ages both in the nursery and in the field (*26*). Invasion of stems by *Phytophthora* spp. initially causes a yellowish-brown discoloration of tissues in the inner bark and cambium. This infection may remain localized and may not be visible externally. When the infection is more extensive, bark tissues crack, disintegrate and exhibit gummosis. In the Sorrento peninsula the brown rot of fruit is a serious problem for the lemon. The disease is also caused by *P. syringae* Carne 1925 (*27*, *28*).

In this paper we describe the primary structure determination of three α-elicitin forms purified from culture filtrates of *P. hibernalis* Carne 1925. We also describe their effects on the usual HR and electrolysis leakage assay (ELA) tests on tobacco (*Nicotiana tabacum*, cv "Rustica") and discuss on their structure-elicitor activity relationships.

MATERIALS AND METHODS

Production of Culture Filtrates—The pathogenic strain of *P. hibernalis* Carne 1925, the causal agent of rot of *citrus lemon* fruits was isolated in the North slope of Sorrento, Italy and deposited in the culture collection at the Department of AR.BO.PAVE University of Naples Federico II. The disease is caused by two *Phytophtora* species, *P. hibernalis* and *P. syringae* (*27*, *28*). The identification of the two different species was confirmed by morpho-biometric characters according to the Tabular Key (*29*). The stock culture of *P. hibernalis* Carne 1925 was maintained on V-8 agar. Liquid cultures were obtained by growing the strain in flasks containing ASYT medium composed of: L-asparagine, 1 g; sucrose, 10 g; yeast extract, 5 g; thiamine, 0.001 g; $KH_2PO_4{\cdot}7H_2O$, 0.5 g; distilled water, 1000 mL. The flasks were incubated and stirred (120 rev/min) for 12 day at $21 \pm 1^{\circ}C$, under the natural alternation of light and dark, then the culture fluid was strained through cheese cloth and filter paper, sterilised by filtration through a 0.22 μm membrane and stored at −20°C until use.

Purification of Hibernalins—Culture filtrates (1 L) were concentrated by evaporation under vacuum to 500 mL, treated with 3 volumes of acetone at −10°C and refrigerated for 2 h (*5*). The mixture was centrifuged (Kendro Laboratory Products, Asheville, NC, USA) at 10,000 rpm for 30 min; the supernatant was evaporated under reduced pressure to remove acetone and then dialyzed using tubes with cut-off 3.5 kDa. The non-permeated fraction was lyophilized, weighed (185 mg),

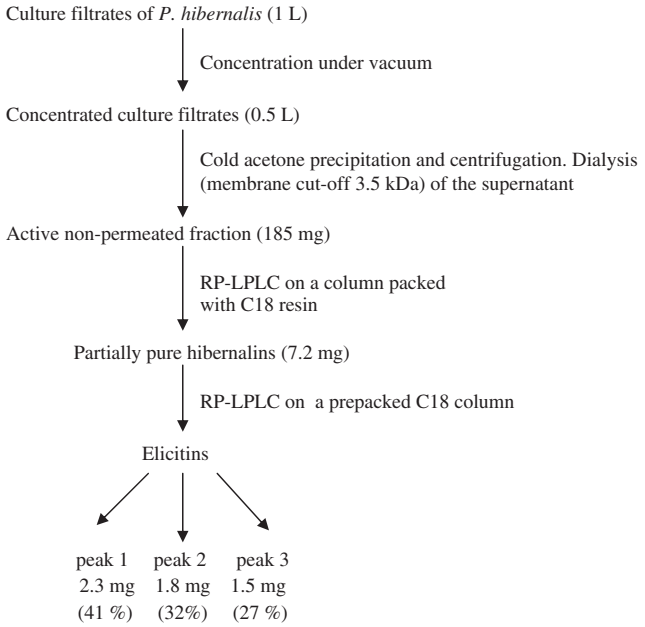

Scheme 1. **Purification procedure of three hibernalin forms.**

and chromatographed on a column (22×1.5 cm) packed with Lichroprep RP-C18 resin (25–40 μm, Merck, Darmstad), and eluted step-wise at flow rate of about 10 mL/min under low pressure with aqueous CH_3CN (0, 10, 20, 30, 40 and 100% CH_3CN in H_2O; ≈200 mL for each step). The elution was monitored at 210 nm, using a spectrophotometer Perkin Elmer, and the eluent changed when the absorbance was below 0.010 OD. The sample eluted at 40% CH_3CN was dried in rotavapor under reduced pressure and lyophilized, obtaining 7.2 mg of partially pure hibernalins. This fraction was further purified at low pressure (3 bar) on a pre-packed Lichroprep RP-C18 column (24×1 cm, 25–40 μm particle) eluted step-wise with aqueous CH_3CN (0, 1, 5, 10, 20, 30, 40, 50 and 100% of acetonitrile in water; 20 mL each step). 2 mL fractions were collected and monitored by UV absorbance at 210 nm. Three main peaks were obtained: peak 1 (2.3 mg), peak 2 (1.8 mg) and peak 3 (1.5 mg) (Scheme 1). The chromatographic behaviour of these three samples was also tested on an analytical RP-HPLC column (Beckman C18 column; 250×4.6 mm; 5 μm particle size) with or without a prior treatment with a denaturing agent (8 M urea) for 24 h, at room temperature. The elution was performed with a continuous gradient (5–50% over 60 min) of aqueous CH_3CN at a flow rate of 1 mL/min.

Cyanogen Bromide Cleavage—Cleavage of the three native elicitin samples with cyanogen bromide was carried out in 70% formic acid as already reported (*30*). At the end of the incubation time CNBr-treated samples were dried over NaOH pellets under vacuum, and *S*-pyridylethylated (see later).

S-*pyridylethylation*—Samples (25 μg) of CNBr-treated peak 1, peak 2 and peak 3 of Fig. 1 were *S*-pyridylethylated as previously reported (*31*) and

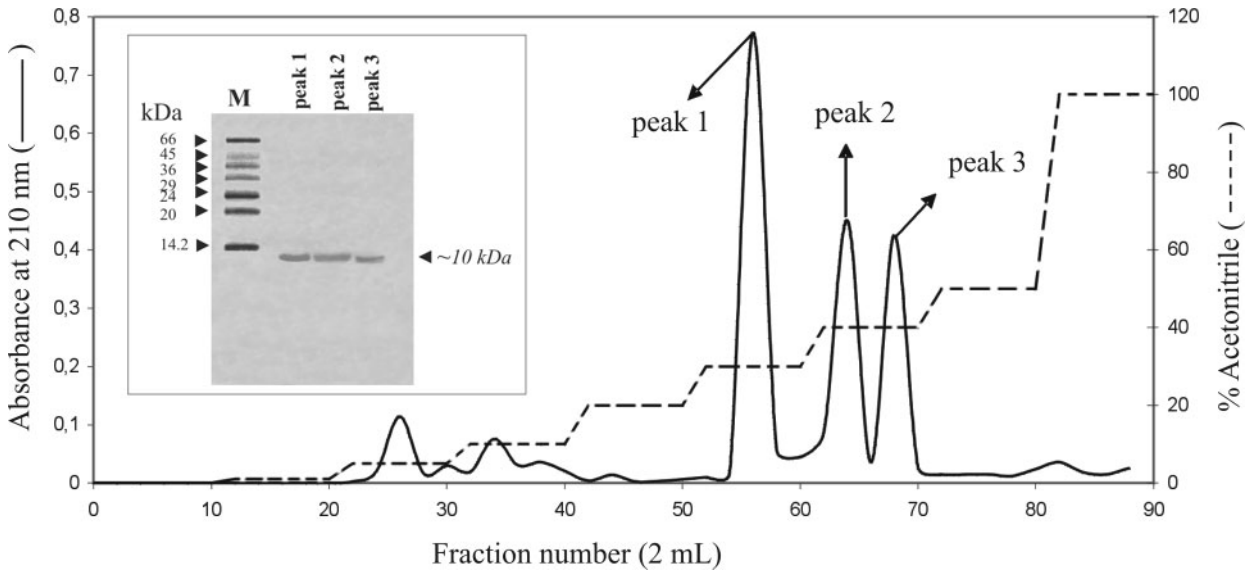

Fig. 1. **Chromatographic profile of culture filtrates of *P. hibernalis* obtained by step-wise elution from an RP-LPLC, C18 column, using aqueous CH_3CN as eluent under low pressure (LP, 3 bar).** Flow rate 4 mL/min; fraction of 2 mL. In the insert, SDS–PAGE analysis of peaks 1–3; M, molecular weight markers; lines 1–3, peaks 1, 2 and 3, respectively. Proteins were detected with silver stain.

chromatographed by RP-HPLC on a Beckman C18 column (250 × 4.6 mm, 5 μm particle size), using a continuous gradient of aqueous CH_3CN containing 0.1% TFA as eluent, at a flow rate of 1 mL/min. Optimal separations were obtained using the following elution conditions: time 0–20 min, 5% B; time 20–66 min, 10% B; time 66–96 min, 28% B; time 96–101 min, 28% B; time 101–181 min, 45% B; time 181–196 min, 95% B.

Amino Acid Sequencing—Native or *S*-pyridylethylated hibernalins were adsorbed on ProSorb™ membranes (Applied Biosystem) and then sequenced by automated Edman degradation on a pulsed phase sequencer (Model 491C; Applied Biosystems) as previously reported (*30*). CNBr-peptides were dried and sequenced in the same way.

Mass Spectrometry of Elicitins and Peptides—Molecular weights of native proteins were obtained by MALDI-TOF-MS Voyager DE-STR (accuracy 50 ppm). Molecular weights of peptides were determined by MALDI-TOF-MS (*32*) and ESI-MS (*33*). Peptide mapping of elicitins was carried out by MALDI-TOF-MS, comparing their experimental masses with those of the peptides which can be theoretically derived from syringicin (*6*). Edman degradation analysis supported the correct fragment assignment.

Preparation of Cross-linked Hibernalin Derivatives—Cross-linked derivatives of elicitins were prepared with DFDNB (Sigma-Aldrich), as previously reported (*34*). Briefly, hibernalin samples (100 μg) were dissolved in 100 μl of 50 mM sodium borate buffer, pH 8.5 (~100 μM elicitins). DFDNB (1 mg/mL) was added to the protein solution to obtain 1:10 or 1:5 [reagent: elicitin(s); mol:mol] ratios. The reaction mixture was stirred for further 24 h in the dark. To stop the reaction, the sample was taken into the loading buffer and analysed by SDS-PAGE (18% polyacrylamide) (*34*).

Gel-filtration Analyses—Gel-filtration was performed on an Amersham Pharmacia Biotech AKTA FPLC, using an Amersham Pharmacia Biotech Superdex™ 75 10/300 GL column. The column was equilibrated with 10 mM Tris.Cl pH 7.2 buffer, containing 0.15 M NaCl. Protein elution was detected by recording the absorption at 214 nm. As molecular weight markers the following proteins were used: bovine serum albumin (BSA; 66 kDa); myoglobin from horse heart (Mb; 17 kDa) and ubiquitin (Ub; 8.5 kDa). A similar experiment was carried out with 30% CH_3CN in water.

Bioinformatics Study On-line 3D-modelling—3D-model of hib1 was obtained using a comparison procedure with known 3D-protein structure available on Swiss-Model server (http://www.expasy.org/swissmod/SWISS-MODEL.html).

HR induction assay—Induction of HR by peaks 1, 2 and 3 of Fig. 1 was determined by infiltrating 100 μL sterile distilled water solutions of proteins (0.26 μM for peak 1 and peak 2 and 0.35 μM for peak 3) into asymptomatic tobacco (*Nicotiana tabacum* L., cv. Rustica grown in greenhouse using environmental conditions) leaves. HR was scored when a brown necrosis occurred in the infiltrated area 48 h after inoculation. To test the induction of distal HR, petiole dip assays (*2*) were carried out on cut tobacco leaves. Leaf petioles were treated with 25 μL of a solution 0.2 μM for peak 1 and peak 2 and 0.35 μM for peak 3. The solution was taken up after about 2 h. Then the leaves were transferred to sterile water. Necrotic lesions were monitored visible after 2 and 7 day and ranked from minute necrotic spots to large, confluent necrotic areas.

ELA Assay—Thirty tobacco leaf discs (5 mm diameter) were incubated for 24 h, in 2 mL of peaks 1, 2 and 3 (0.1 mg/mL) and distilled water (*35*). After the incubation six leaf disks were transferred to sterile distilled water (15 mL) and the corresponding conductance was measured in μS using a conductivity meter with 20 electrodes (range 20–200 mS/cm; K = 1) connected to a computer with a specific program. Each value was the mean of at least five replicated samples and was calculated as the difference from the reading at the beginning of the assay, after several hours. The test was repeated twice.

UniProt Knowledgebase Accession Numbers—The primary structure of hibernalin 1 has been deposited in the UniProtKB (accession code P85174).

RESULTS AND DISCUSSION

Elicitin Forms Purification and Primary Structure Determination of hib1 by Edman degradation—The purification of the three elicitins from culture filtrates of *P. hibernalis* Carne 1925 was performed applying a modified procedure (Scheme 1) with respect to that previously reported for syringicin (*6*). In particular, the gel-filtration step of the non-permeated lyophilized supernatant, obtained after dialysis, was replaced with the RP-LPLC step on a column packed with C18 resin, eluted step-wise with increasing concentration of aqueous CH_3CN. A biologically active fraction was obtained at 40% CH_3CN (data not shown). This crude fraction was re-chromatographed by RP-LPLC on a commercial RP-C18 column (*6*), giving rise to three distinct peaks (Fig. 1). In particular, peak 1 (2.3 mg; 41%) was eluted at 30% CH_3CN, while peaks 2 (1.8 mg; 32%) and 3 (1.5 mg; 27%) were eluted at 40% of the same eluent.

The reported purification procedure, based on two consecutive chromatographic steps under reduced pressure is reported for the first time for the purification of elicitins from *Phytophthora* species.

The three peaks were analysed by SDS-PAGE (see insert of Fig. 1), which revealed, in all three samples, the presence of a single protein band with the same molecular weight of about 10 kDa.

The apparently homogeneous elicitins were then reduced, *S*-pyridylethylated and their N-terminal amino acid sequences determined. This analysis allowed us to obtain the sequence of the first thirty N–terminal amino acid residues (TTCTTTQQTA AYVALVSILS DSSFNQCATD), identical for all three proteins and, in turn, identical to the N-terminal of syringicin, the α-elicitin from *P. syringae* (*6*).

In order to explain the different elution volumes of the three peaks, from the RP-LPLC column (Fig. 1) which, in general, separates analytes on the basis of their hydrophobic properties, we decided: i) to determine the molecular weight of the samples of peaks 1–3 by mass spectrometry; ii) to complete the amino acid sequence of peak 1 (the major form) and, iii) to characterize, by mass spectrometry mapping, the protein component of peak 2 and peak 3.

To obtain the molecular weight value, we first used the ESI-MS, which provided a M_r for peak 1 of 10,194.9 ± 0.2. In the case of peak 2 and peak 3 no results were obtained, likely because the correspondent samples polymerised in the mass spectrometry capillary, which was even blocked. We then decided to use the MALDI TOF-MS which provided the following M_r values: 10,194.82 for peak 1 [relative mass intensity (RI) 100%]; 10,194.86 and 10,209.33 for peak 2 (two forms; 100 and 78% RI, respectively), and 10,194.87, 10,209.47 and 10,223.80 for peak 3 [three forms; (100, 90 and 40% RI, respectively)]. Multiple values (about 20,000, 30,000 and 40,000 M_r, data not shown) were also seen, consistent with the presence of higher aggregated forms.

These results revealed that peak 1 contained a homogeneous protein (hereafter called hib1), while peak 2 contained hib1 and a molecular component with M_r 10,209.47 (hereafter called hib2), and peak 3 contained hib1, hib2 and a component with M_r 10,223.80 (hereafter called hib3).

From the results obtained so far we concluded that the molecular mass differences among the three forms, with the same primary structure up to residue 30, was due to differences in the remaining part of the molecule.

Sequence Determination of hib1—Since hib1 present in peak 1 of Fig.1 was homogeneous, judging from the MS data, we decided to complete its sequence, to obtain a reference sample. Native hib1 was treated with several proteases, commonly employed to obtain peptides for sequence determination purposes, but, in all cases, no fragmentation was achieved, revealing a remarkable resistance of hib1 to proteolytic agents. Therefore, hib1 was subjected to chemical cleavage by CNBr and then reduced and *S*-pyridylethylated. The obtained peptides were solubilized in 50% formic acid and separated by RP-HPLC, applying the elution program reported in Materials and Methods (Fig. 2, peak 1). CNBr peptides from hib1 were sequenced by automated Edman degradation and provided a sequence set of 98 amino acid residues (Table 1). In particular, peptides CB-1/CB-2, CB-3/CB-4 and CB-6/CB-7 were present as doublets, due to the homoserine/homoserine lactone equilibrium at their C-terminus. Peptide CB-5 corresponded to the C-terminal peptide of the protein (residues 60–98). The peptide corresponding to the amino acid residues 51–59 was not found, likely because adsorbed to the reverse phase column, or eluted in the flow-through of the same column, which contained peptide solvent (formic acid) and residual reagents. Peptides CB-1/CB-2 corresponded to the amino acid residues 36–59 with Met in position 50, as shown by Edman degradation.

CNBr peptides were obtained with different yields (Fig. 2), likely as a consequence of several factors: i) differences in CNBr cleavage efficiency at the three methionyl residues at positions 35, 50 and 59, respectively; ii) occurrence of the homoserine-homoserine lactone equilibrium at the C-terminus of peptides CB-1/2, CB-3/4 and CB-6/7; iii) differential peptide solubility and, iv) differential adsorption of peptides to the RP C18 column.

Furthermore, the presence of Met at position 50 of peptides CB-1/2 was unexpected, but it could be explained considering that the pyridylethylation of the

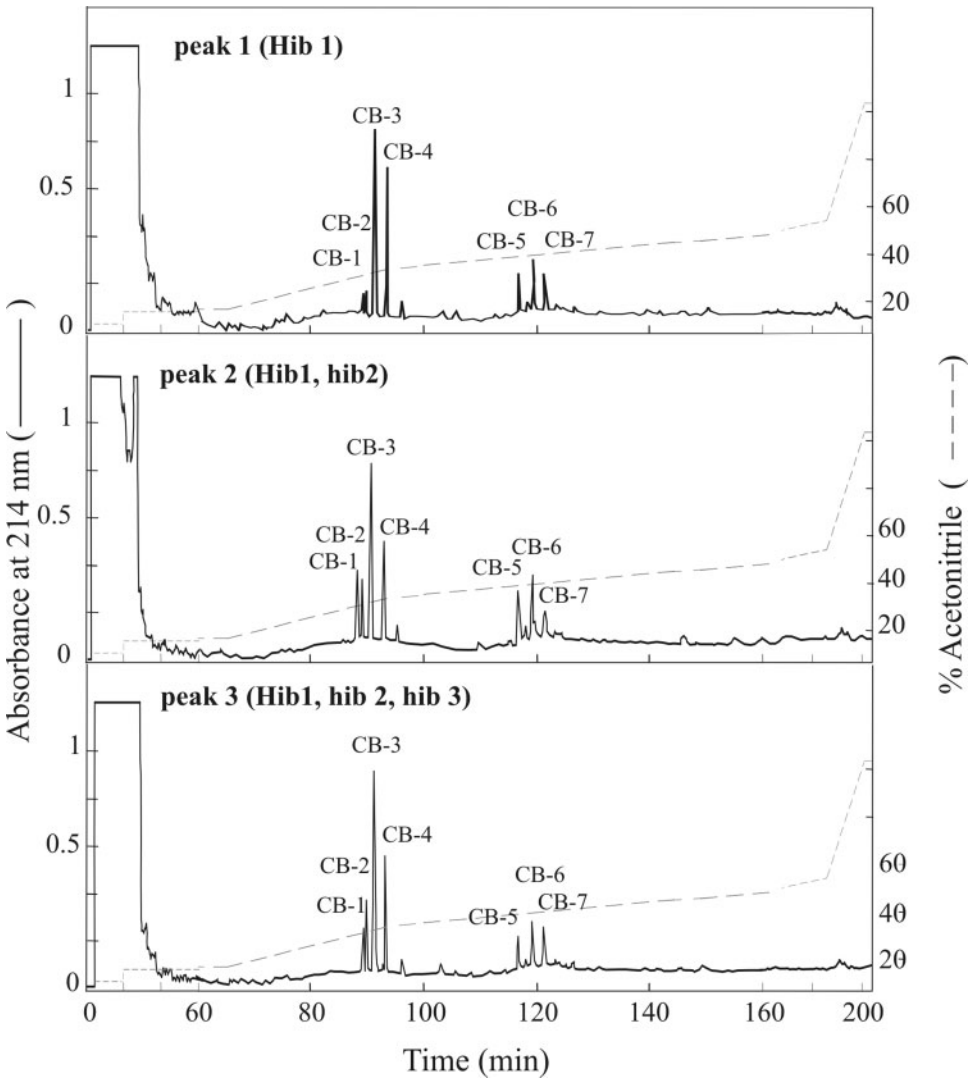

Fig. 2. **RP-HPLC separation of *S*-pyridylethylated peptides obtained by CNBr cleavage of peaks 1, 2 and 3 of Fig. 1.**

cysteinyl residues was performed in the presence of thiol excess, which is known to revert Met-sulphoxide to Met [(*36*); Fig. 3B]. Finally, the complete amino acid sequence of hib1 (Fig. 3A) was obtained aligning the CB-peptides and using syringicin as reference protein, whose N-terminal sequence had already been shown to be identical to the N-terminal sequence of hib1 (see above).

The molecular mass of hib1, obtained from the sequence was 10,194.62. This value was identical, within the experimental error, to that experimentally determined by ESI-MS and MALDI-TOF-MS and in turn to that of syringicin (*6*).

Characterization of Peaks 2 and 3 with MALDI-TOF-MS—Once obtained the sequence of hib1, the major elicitin form, we undertook the structural characterization of the component(s) of peaks 2 and 3 of Fig. 1 and adopted a different, more sensitive approach, based on mass spectrometry, which is particularly useful in the case of mixture samples.

To directly verify possible differences in the amino acid sequence of their protein components, peaks 2 and 3 were cleaved with CNBr, followed by pyridylethylation of the cysteinyl residues. The resulting RP-HPLC chromatograms are reported in Fig. 2. Comparing the three chromatograms of Fig. 2, it appears that, while the elution patterns are identical each other, differences are mainly related to peak heights, especially in the case of peaks 1–4. The eluted peptides were then individually analyzed by MALDI-TOF-MS, which confirmed, on the basis of the comparison between experimental and theoretical molecular weights, the presence, also in peaks 2 and 3, of all CNBr peptides of hib1 (Table 2). Quantitative differences were related only to peptides CB-1/CB-2, which, submitted to Edman degradation, confirmed the sequence LTATALPTTAQYKLMCASTACKTHse, corresponding to the trait 36–59 of hib1.

The results presented above showed that CNBr did not cleave efficiently after Met 50. In fact, the percentage of

Table 1. **Amino acid sequences of *S*-pyridylethylated hib1 and of CNBr peptides of Fig. 2A, used to assemble the complete amino acid sequence.**

Protein/peptide	Sequence	Notes
Hib1, hib2 and hib3	1 TTCTTTQQTA AYVALVSILS DSSFNQCATD 30	*S*-Pyridylethylated protein; N-terminal (1–30)
CB-1	36 LTATALPTTA QYKLMCASTA CKTHse 59	No cleavage at the internal Met. Homoserine form
CB-2	36 LTATALPTTA QYKLMCASTA CKTHse> 59	No cleavage at the internal Met. Homoserine lactone form
CB-3	36 LTATALPTTA QYKLHse 50	Homoserine form
CB-4	36 LTATALPTTA QYKLHse> 50	Homoserine lactone form
CB-5	68 ITKIVSLNAP DCELTVPTSG LVLNVYSYAN GFSSTCASL 98	C-terminal peptide
CB-6	1 TTCTTTQQTA AYVALVSILS DSSFNQCATD SGYSHse 35	N-terminal peptide. Homoserine form
CB-7	1 TTCTTTQQTA AYVALVSILS DSSFNQCATD SGYSHse> 35	N-terminal peptide. Homoserine lactone form

peptides CB-1 plus CB-2 (residue 36–59, with internal intact Met 50) was lower in hib1 (about 12%), and higher in hib2 (25%) and hib3 (27%) (Fig. 2).

Indeed, peptide 36–59 was produced in lower quantity from peak 1 (hib1), and in higher amounts from peak 2 and peak 3 of Fig. 1. As a counterpart, the amount of peptide 36–50 (peaks CB-3 and CB-4; Fig. 2) was higher from peak 1 (hib1) than from peaks 2 and 3. One explanation of the resistance to CNBr cleavage could be the oxidation of Met to Met-sulphoxide or sulphone (Fig. 3). Therefore, the presence of peaks CB-1 and CB-2 (Fig. 2) could depend both from a low cleavage yield and from the fact that Met had been transformed to sulphone which could not be reverted to methyonine, while part of the sulphoxide had been transformed to Met, which appeared during the Edman degradation. The data pointed to the fact that peaks 2 and 3 of Fig. 1 contained hib1 (as in peak 1), and modified (oxidized) forms at Met 50 (see later). This conclusion is supported by the M_r values found, by MALDI-MS, in peaks 2 and 3, which differ each other of about 16 uma (see earlier). This value should correspond to the oxidation of Met to the corresponding sulphone (+16 uma) and then sulphoxide (further +16 uma). Thus, the oxidation could explain the different M_r values of the three elicitin forms and, considering also the likely aggregation, the different elution times from the RP-LPLC column (Fig. 1).

The transformation of Met is a dynamic process and apparently oxidised Met forms were present in all peaks shown in the chromatogram of Fig. 1 at the time the proteins were treated with CNBr. In addition, the MS analysis of peaks 2 and 3 showed the presence of more than one molecular form. The coexistence of these forms could be likely promoted by conformation changes (denaturation) due to the oxidation of Met, which may have favoured the aggregation during the purification steps performed in the presence of CH_3CN.

This issue was examined by gel-filtration on the FPLC system as reported in Materials and Methods. To exclude the possibility of interactions between hibernalins and the gel support, 0.15 M NaCl was added to the aqueous buffer at pH 7.2. Furthermore, 30% CH_3CN (the maximum percentage allowed on Superdex resins, as

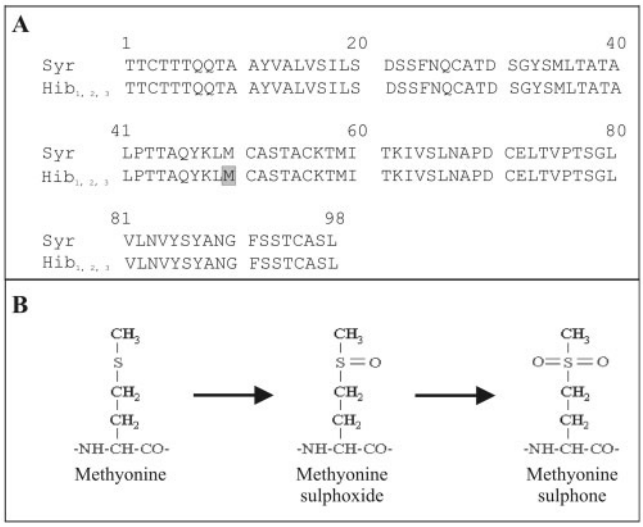

Fig. 3. **(A) Amino acid sequence of hib1, hib2 and hib3. The sequence is identical to that of syringicin.** The suggested, oxidized methionyl residue is shaded; (B) scheme of the oxidative steps, occurring on the Met sulphur.

suggested by the manufacturer) was added. These conditions simulated those of the RP-HPLC chromatography. The chromatographic profile of samples of peaks 1, 2 and 3 of Fig. 1 from the analytical Superdex 75 column in 10 mM Tris·Cl, 0.15 M NaCl, pH 7.2 or 30% CH_3CN in water are reported in Fig. 4A–C and 4D–F, respectively. The obtained results indicated the presence of dimeric forms ($\sim M_r$ 20,000) in all samples when the elution was performed with 10 mM Tris·Cl, 150 mM NaCl, pH 7.20, in equilibrium with oligomeric forms ($M_r > 40{,}000$) in the presence of 30% CH_3CN with elution volumes of 8.51 and lower, 8.08 and 7.78 mL for hib1 (peak 1), hib1/hib2 (peak 2) and hib1, 2 and 3 (peak 3), respectively (Fig. 4D–F).

Furthermore, to investigate the influence of denaturing agents on the hibernalin forms, peaks 1, 2 and 3 were also treated with urea and then analysed by analytical RP-HPLC. It was found (Fig. 5) that their chromatographic behaviour, without and with treatment with 8 M urea, presented no differences in

Table 2. **Peptide mapping by MALDI-TOF mass spectrometry of peak 1, peak 2 and peak 3 of Fig. 1 after CNBr cleavage.**

Peptide	Experimental M_r			Syringicin derived peptides	Sequence position	Notes
	Peak 1	Peak 2	Peak 3			
CB-1	2701.6	2701.5[a]	2701.3	2701.2[b]	36–59	
CB-2	2683.6	2683.7[a]	2683.5	2682.3[c]	36–59	
CB-3	1592.8[b]	1592.9[b]	1593.0[b]	1591.9[b]	36–50	
CB-4	1574.8[c]	1575.2[c]	1575.0[c]	1573.9[c]	36–50	
CB-5	4260.6	4260.4	4260.4	4259.1	60–98	C-terminal
CB-6	3847.9	3848.0	3848.1	3846.7[b]	1–35	N-terminal
CB-7	3830.0	3829.8	3829.9	3828.7[c]	1–35	N-terminal

Theoretical molecular weights of peptides from CNBr-treated syringicin are reported for comparison. The molecular weights take into account the pyridylethylation reaction. CB, cyanogen bromide peptides. The mass values have been reported as average of the different values obtained by each MS analysis (three determinations).
[a]Present in trace. [b]Peptides with C-terminal homoserine. [c]Peptides with C-terminal homoserine lactone.

elution times, but only a widening of peaks 2 and 3 (inserts D and F, without and with denaturation, respectively). These results give additional evidence regarding the occurrence of protein aggregates for peaks 2 and 3 that are somewhat very resistant also to denaturation.

Furthermore, to establish the presence of more than one molecular form in peaks 2 and 3, we decided to covalently stabilize them. For this purpose, samples were reacted with the cross-linking agent DFDNB. In the presence of DFDNB at 1:10 ratio [reagent: hibernalin(s)] no dimerization was present in hib1 (peak 1), up to 24 h (data not shown). In the same conditions, oligomeric forms were present when hib1 was in association with hib2 (peak 2) or with hib2 and 3 (peak 3). Furthermore, doubling the DFDNB concentration [ratio 1:5; reagent: hibernalin(s)] the oligomeric forms (dimer, trimer and higher forms) increased (Fig. 6). Although not reliable, due to the potential artifactual nature of the observed results, the cross-linking experiment was carried out to further support the tendency of hibernalins, under certain conditions, to aggregate.

A possible mechanism for the aggregation of the three hibernalins is suggested in Fig. 7. The homogeneous hib1 is progressively oxidized to hib2 (Met50 sulphoxide derivative) and hib3 (Met50 sulphone derivative) (see also Fig. 3B), undergoing to conformational change(s), which increase the association propensity, giving rise to the hib1/hib2 heterodimer (peak 2 of Fig. 1) and to the heterotrimer hib1/hib2/hib3 (peak 3 of Fig. 1). Very likely, the formation of other polymeric forms is possible, but they were not detected in the chromatograms of Fig. 1.

In previous studies (*6*), purified syringicin preparations from *P. syringae* contained neither oxidized nor oligomeric forms. It is conceivable to suggest that these forms, observed in the present study, could derive from a longer exposure to CH_3CN during the isolation procedure, and that the denaturation induced by CH_3CN might speed up or favour the oxidation of Met 50.

Biological Activity of the Three Hibernalins—The biological characterization of the chromatographic peaks 1, 2 and 3 from Lichroprep RP- C18 column

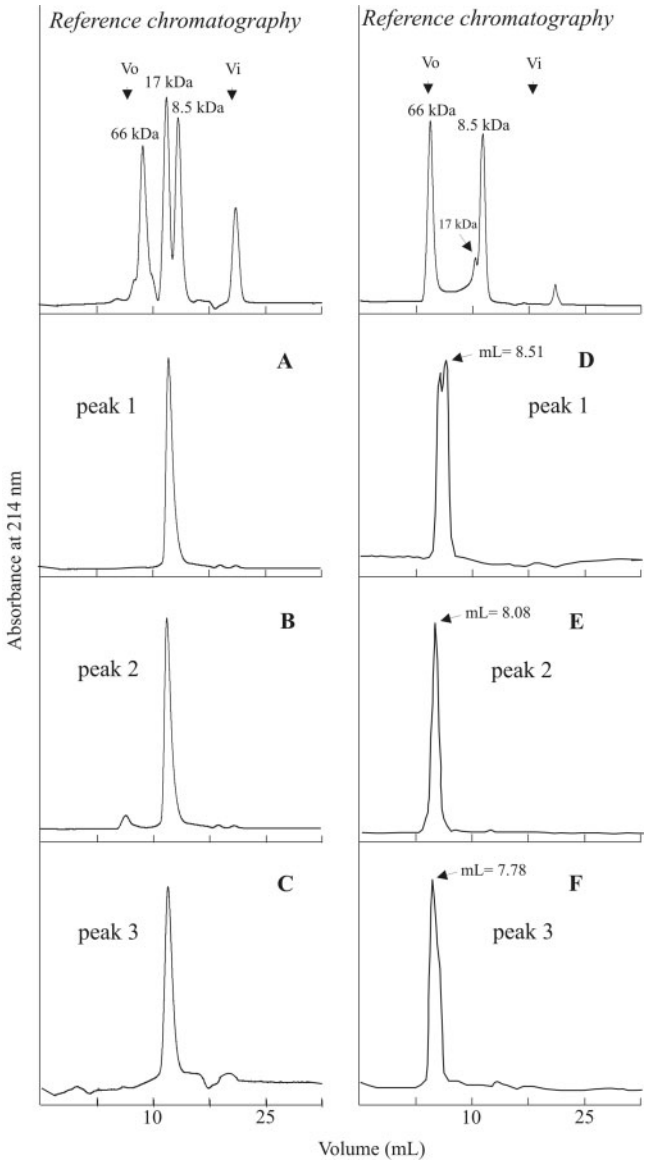

Fig. 4. **Elution profile from the analytical chromatography on Superdex 75 of peaks 1, 2 and 3 of Fig. 1.** (A–C) Separation in aqueous buffer, respectively; (D–F) separation in 30% acetonitrile, respectively.

(see Fig. 1) was also performed by the distinct HR induced on *Nicotiana tabacum* cv "Rustica" (*17*, *37*) and ELA (*35*).

The first test showed that hib1 (peak 1) induced chlorotic stains up to the 5° leaf, peak 2 up the 4° and peak 3 induced no response. Pure hib1 induced a response stronger than in association with hib1/hib2 (peak 2) and with hib1/hib2/hib3 (peak3).

In the second test, hib1 induced a statistically different increase of the conductivity in comparison to peaks 2

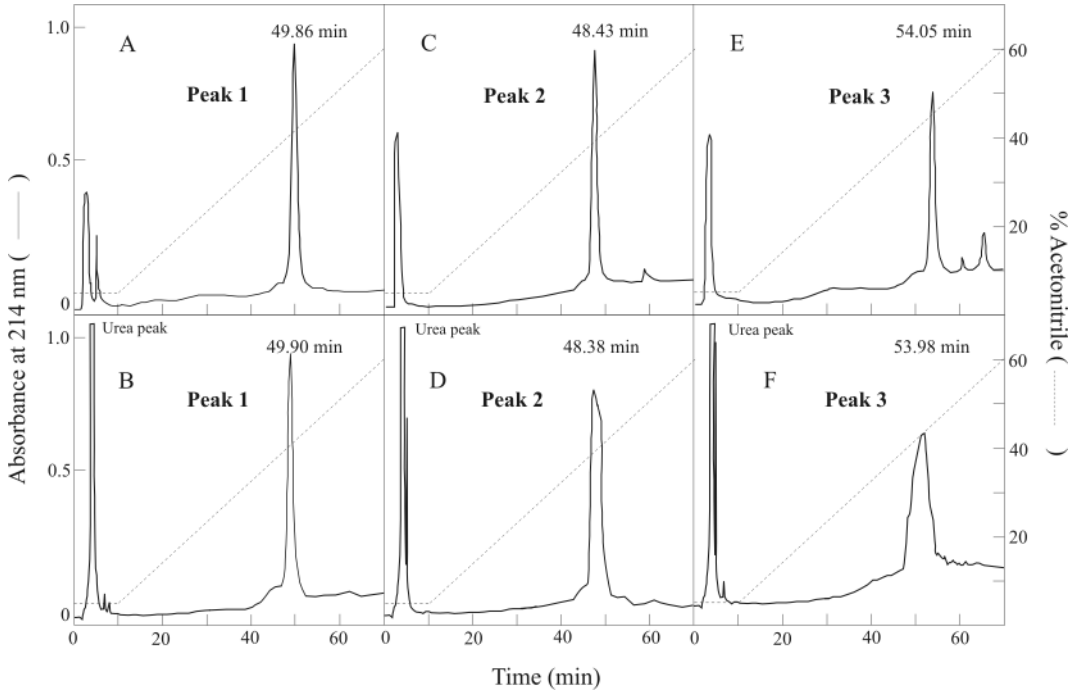

Fig. 5. **RP-HPLC analysis of peaks 1–3 of Fig. 1 without or with an incubation in the presence of 8 M urea, for 24 h at room temperature.** The chromatographic profiles are reported for peak 1, peak 2 and peak 3 without (panels A, C and E) and with (B, D and F) the incubation in the presence of urea, respectively.

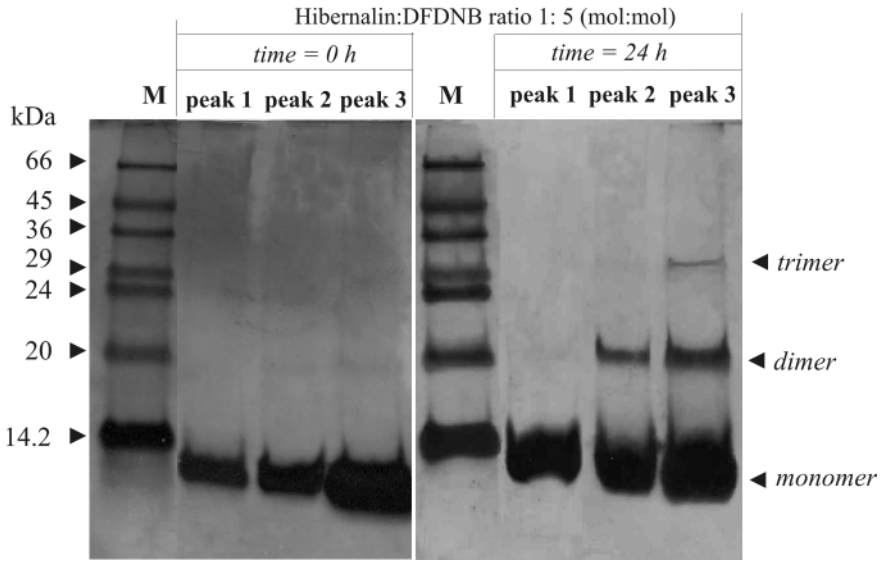

Fig. 6. **SDS–PAGE analysis of the peaks 1–3 of Fig. 1, after incubation with DFDNB (reagent : protein ratio 1:5).** M, molecular weight markers; lines 1–3, peak 1, peak 2 and peak 3, respectively at 0 h incubation; lines 5–7, peak 1, peak 2 and peak 3, respectively, after 24-h incubation.

and 3, these latter giving any type of response (Fig. 8). These results underline only a correlation between ELA and HR for hib1 (peak 1).

The different activity of the three hibernalin peaks could be explained considering both the presence of oligomeric forms and the oxidation of Met 50.

Once oxidized, this residue could prevent its correct location inside the core changing the 3D structure of the protein. Probably, oxidized Met remains outside and drags other hydrophobic residues outside leading to local conformational modifications which favour aggregation in oligomeric inactive forms (*23*, *38*). This hypothesis is also supported by previous NMR studies (*39*), which revealed the occurrence, in cryptogein of an unusual hydrophobic core comprising a cluster of three methionines (Met 35, Met 50, Met 59). It is also suggested that these residues can affect the stability of the protein, justifying also their high conservativity.

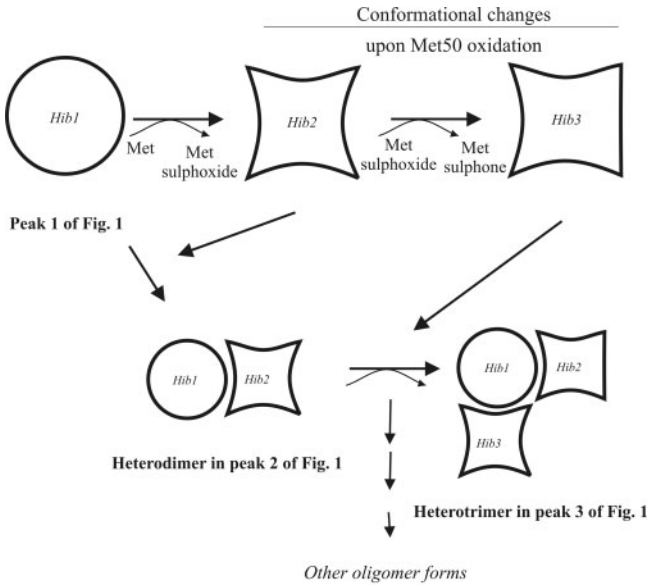

Fig. 7. **Hypothesized mechanism for self-aggregation of hib1, hib2 and hib3 upon Met 50 oxidation.** The stechiometry of the protein forms in the oligomer does not correspond to the real situation.

CONCLUSION

This paper describes for the fist time the characterization of hib1, an α-elicitin isolated from culture filtrates of *P. hibernalis*. Hib1 shows the same primary structure and activity of syringicin, α-elicitin isolated from *P. syringae*, as revealed by biochemical analysis and biological assays (HR and ELA).

Moreover, two oligomeric forms hib1/hib2 (peak 2) and hib1/hib2/hib3 (peak 3) were isolated and characterized; these forms are likely due to the oxidation of a Met residue (Met 50), to sulphoxide and than to sulphone. The oligomeric forms did not show biological activity.

In perspective, the analysis of these oxidized forms may give useful insights into structure-elicitor activity relationships of the elicitins.

This work was supported by funds from the Second University of Naples and University of Naples Federico II, Italy. DiSSPAPA contribution n° 156. Antonino Testa's position was funded by the Italian Ministry of Education (MIUR), project "Rientro dei Cervelli", of the University Politecnica delle Marche, Ancona, Italy.

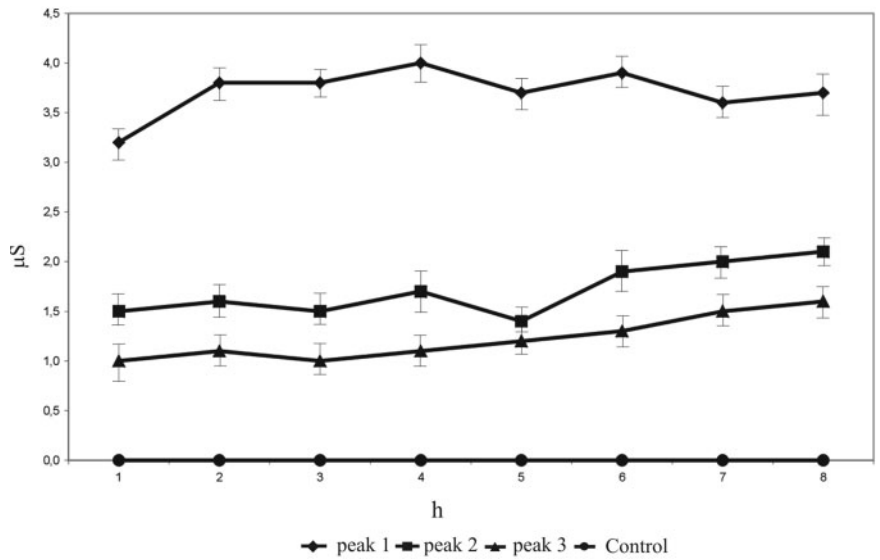

Fig. 8. **ELA curves stimulated by the three hybernalins on tobacco leaf disks**. Results are mean values of five replicates ± SD. The test was repeated twice.

REFERENCES

1. Kamoun, S. (2001) Nonhost resistance to *Phytophthora*: novel prospects for a classical problem. *Curr. Opin. Plant Biol.* **4**, 295–300
2. Huet, J.C., Nespoulous, C., and Pernollet, J.C. (1992) Structures of elicitin isoforms secreted by *Phytophthora drechsleri*. *Phytochemistry* **31**, 1471–1476
3. Nespoulous, C., Huet, J.C., and Pernollet, J.C. (1992) Structure-function relationship of Alpha-elicitin and beta-elicitin, signal proteins involved in the plant-*Phytophthora* interaction. *Planta* **186**, 551–557
4. Ricci, P., Bonnet, P., Huet, J.C., Sallantin, M., Beauvais-Cante, F., Bruneteau, M., Billard, V., Michel, G., and Pernollet, J.C. (1989) Structure and activity of proteins from pathogenic fungi Phytophthora eliciting necrosis and acquired resistance in tobacco. *Eur. J. Biochem.* **183**, 555–563
5. Capasso, R., Cristinzio, G., Evidente, A., Visca, C., Ferranti, P., Del Vecchio-Blanco, F., and Parente, A. (1999) Elicitin 172 from an isolate of *Phytophthora nicotianae* pathogenic to tomato. *Phytochemistry* **50**, 703–709
6. Capasso, R., Cristinzio, G., Di Maro, A., Ferranti, P., and Parente, A. (2001) Syringicin, a new alpha-elicitin from an isolate of *Phytophthora syringae*, pathogenic to citrus fruit. *Phytochemistry* **58**, 257–262
7. Churngchow, N. and Rattarasarn, M. (2000) The elicitin secreted by *Phytophthora palmivora*, a rubber tree pathogen. *Phytochemistry* **54**, 33–38
8. Huet, J.C. and Pernollet, J.C. (1989) Amino acid sequence of cinnamomin, a new member of the elicitin family, and its comparison to cryptogein and capsicein. *FEBS Lett.* **257**, 302–306
9. Koehl, J., Osswald, W., Khon, H., Elstner, E.F., and Heiser, I. (2003) Different responses of two tobacco cultivars and their cell suspension cultures to quercin, a novel elicitin from *Phytophthora quercina*. *Plant Physiol. Biochem.* **41**, 261–269
10. Ponchet, M., Panabieres, F., Milat, M.L., Mikes, V., Montillet, J.L., Suty, L., Triantaphylides, C., Tirilly, Y., and Blein, J.P. (1999) Are elicitins cryptograms in plant-Oomycete communications? *Cell. Mol. Life Sci.* **56**, 1020–1047
11. Panabieres, F., Ponchet, M., Allasia, V., Cardin, L., and Ricci, P. (1997) Characterization of border species among Pythiaceae: several Phytium isolates produce elicitins, typical proteins from Phytophthora spp. *Mycol. Res.* **101**, 1459–1468
12. Huet, J.C., Le Caer, J.P., Nespoulous, C., and Pernollet, J.C. (1995) The relationship between the toxicity and the primary and secondary structures of elicitinlike protein elicitors secreted by phytopathogenic fungus Pythium vexans. *Mol. Plant Microbe In.* **8**, 302–310
13. Ricci, P., Trentin, F., Bonnet, P. Venard, P., Mouton-Perronnet, F., and Bruneteau, M. (1992) Differential production of parasiticien an elicitor of necrosis and resistance in tobacco, by isolates of *Phytophthora parasitica*. *Plant Pathol.* **41**, 298–307
14. Wang, Y.C., Hu, D.W., Zhang, Z.G., Ma, Z.C., Zheng, X.B., and Li, D.B. (2003) Purification and immunocytolocalization of a novel *Phytophthora boehmeriae* protein inducing the hypersensitive response and systemic acquired resistance in tobacco and Chinese cabbage. *Physiol. Mol. Plant. Pathol.* **63**, 223–232
15. Bonnet, P., Bourdon, E., Ponchet, M., Blein, J.P., and Ricci, P. (1996) Acquired resistance triggered by elicitins in tobacco and other plants. *Eur. J. Plant Pathol.* **102**, 181–192
16. Milat, M.L., Ricci, P., and Blein, J.P. (1991) Capsidiol and ethylene production by tobacco cells to elicitors from *Phytophthora cryptogea*. *Phytochemistry* **30**, 2171–2173
17. Zimmermann, S., Franchisse, J.M., Thomine, S., Barbier Brygoo, H., and Guern, J. (1998) Elicitor-induced chloride efflux and anion channels in tobacco cell suspensions. *Plant Physiol. Biochem.* **36**, 665–674
18. Kamoun, S., Klucher, K.M., Coffey, M.D., and Tyler, B.M. (1993) A gene encoding a host-specific elicitor protein of Phytophthora parasitica. *Mol. Plant Microbe In.* **6**, 573–581
19. Nes, W.D. (1987) Biosynthesis and requirement for sterols in the growth and reproduction of Oomycetes. *ACS Symp. Ser.* **325**, 304–328
20. Ko, W.H. (1986) Sexual reproduction of *Pythium aphanidermatum*: stimulation by phospholipids. *Phytopathology* **76**, 1159–1160
21. Mikes, V., Blein, J.P., Milat, M.L., Ponchet, M., and Ricci, P., (1998) Use of elicitins as lipid carriers and their medical use. International patent, 31 pp. Coden: PIXXD2.
22. Wendehenne, D., Binet, M.N., Blein, J.P., Ricci, P., and Pugin, A. (1995) Evidence for specific, high-affinity binding sites for a proteinaceous in tobacco plasma membrane. *FEBS Lett.* **374**, 203–207
23. Osman, H., Vauthrin, S., Mikes, V., Milat, M.L., Panabieres, F., Marais, A., Brunie, S., Maume, B., Ponchet, M., and Blein, J.P. (2001) Mediation of elicitin activity on tobacco is assumed by elicitin-sterol complexes. *Mol. Biol. Cell* **12**, 2825–2834
24. Buhot, N., Douliez, J.P., Jacquemard, A., Marion, D., Tran, V., Maume, B.F., Milat, M.L., Ponchet, M., Mikes, V., Kader, J.C., and Blein, J.P. (2001) A lipid transfer protein binds to a receptor involved in the control of plant defence responses. *FEBS Lett.* **509**, 27–30
25. Blein, J.P., Coutos-Thevenot, P., Marion, D., and Ponchet, M. (2002) . From elicitins to lipid-transfer proteins: a new insight in cell signalling involved in plant defence mechanisms. *Trends Plant Sci.* **7**, 293–296
26. Gregory, P.H. (1983) Structure of β-cinnamomin, a protein toxic to some plant species in *Phytophthora: Its Biology, Taxonomy, Ecology, & Pathology* (Erwin, ?.C., Bartnicki-Garcia, S., and Tsao, P.H., eds.) pp. 190–192 The Amer. Phytopath. Soc., St Paul, Minn
27. Verneau, R. (1954) Le Phytophthorae parasite degli agrumi nella Campania. **8**, 133–162.
28. Cristinzio, G. (1994) Brown rot of lemon caused by Phytophthora spp. In the Sorrento peninsula. *Petria* **4**, 123–130
29. Stamps, D.J., Waterhouse, G.M., Newhook, F.J., and Hall, G.S. (1990) *Revised tabular key to the species of Phytophthora* C.A.B International Mycological Institute, Mycological Papers
30. Parente, A., Verde, C., Malorni, A., Montecucchi, P., Aniello, F., and Geraci, G. (1993) Amino-acid sequence of the cooperative dimeric myoglobin from the radular muscles of the marine gastropod *Nassa mutabilis*. *Bioch.. Bioph. Acta* **1162**, 1–9
31. Scudiero, R., Capasso, C., Del Vecchio-Blanco, F., Savino, G., Capasso, A., Parente, A., and Parisi, E. (1995) Isolation and primary structure determination of a metallothionein from *Paracentrotus lividus* (*Echinodermata, Echinoidea*). *Comp. Biochem. Physiol. B-Biochem. Molec. Biol.* **111**, 329–336
32. Facchiano, A.M., Costantini, S., Di Maro, A., Panichi, D., Chambery, A., Parente, A., Di Gennaro, S., and Poerio, E. (2006) Modeling the 3D structure of wheat subtilisin/chymotrypsin inhibitor (WSCI). Probing the reactive site with two susceptible proteinases by time-course analysis and molecular dynamics simulations. *Biol. Chem.* **387**, 931–940
33. Chambery, A., De Donato, A., Bolognesi, A., Polito, L., Stirpe, F., and Parente, A. (2006) Sequence determination of lychnin, a type 1 ribosome-inactivating protein from *Lychnis chalcedonica* seeds. *Biol. Chem.* **387**, 1261–1266

34. Adinolfi, S., Piccoli, R., Sica, F., and Mazzarella, L. (1996) BS-RNase tetramers: an example of domain-swapped oligomers. *FEBS Lett.* **398**, 326–332
35. Cristinzio, G. and Saccardo, F. (1994) A rapid technique for screening genetic resistance to *Phytophthora nicotianae* in the genus *Lycopersicon*. *J. Genetic Breeding* **48**, 201–202
36. Houghten, R.A. and Li, C.H. (1983) Reduction of sulfoxides in peptides and proteins. *Method Enzymol.* **91**, 549–559
37. Ricci, P. (1997) Interaction of hypersensitive response (HR), & systemic acquired resistence (SAR) by fungal proteins: the case of elicitins in *Plant Microbe Interactions* (Styacey, G. and Keen, N.T., eds.) Vol. 3, pp. 53–75 Chapman and Hall, New York
38. Lochman, J., Kasparovsky, T., Damborsky, J., Osman, H., Marais, A., Chaloupkova, R., Ponchet, M., Blein, J.P., and Mikes, V. (2005) Construction of cryptogein mutants, a proteinaceous elicitor from *Phytophthora*, with altered abilities to induce a defense reaction in tobacco cells. *Biochemistry* **44**, 6565–6572
39. Gooley, P.R., Keniry, M.A., Dimitrov, R.A., Marsh, D.E., Keizer, D.W., Gayler, K.R., and Grant, B.R. (1998) The NMR solution structure and characterization of pH dependent chemical shifts of the beta-elicitin, cryptogein. *J. Biomol. NMR* **12**, 523–534